

Distribution of proton spectroscopic strengths in the odd-*A* Rb isotopes

G. S. F. Stephans,* H. T. Fortune, L. C. Bland,† M. Carchidi,‡ R. Gilman,§ G. P. Gilfoyle,** and J. W. Sweet
Department of Physics, University of Pennsylvania, Philadelphia, Pennsylvania 19104

(Received 5 January 1987)

The $^{78,80,82}\text{Kr}(^3\text{He},d)$ reactions have been used to measure proton spectroscopic factors for many low-lying levels in $^{79,81,83}\text{Rb}$. Summed spectroscopic strengths and the distributions of strength among states are compared to recent theoretical predictions. The spreading of strength is found to be less than predicted, especially for the $2p_{1/2}$ and $1g_{9/2}$ orbitals.

INTRODUCTION

The odd-*A* Rb isotopes occupy an interesting region for the application of nuclear structure models coupling one (or more) valence particles to the states of a core. Full shell-model calculations are impractical due to the presence of many closely spaced valence orbitals for the protons. This abundance of available orbitals tests the ability of particle-core coupling models to adequately describe a relatively complex level scheme. In addition, the structure of the Kr core varies from roughly vibrational at the $N=50$ closed core (^{86}Kr) to highly rotational for the lighter isotopes ($^{78,80}\text{Kr}$). Any successful model must be able to describe the effect of this transition on the coupling between the core states and the odd proton.

Single-particle spectroscopic factors are an important basic component in any attempt to understand the structure of odd-*A* nuclei. Many models of such nuclei require single-particle orbital occupancies, obtained from the sum of spectroscopic factors, as input parameters. In addition, the spectroscopic factors of individual states can be calculated from relatively simple features of the wave functions rather than from interferences between many different components and thus can serve as a lowest-order check of any model.

Proton spectroscopic factors for many levels in $^{79,81,83}\text{Rb}$ have been measured using the $^{78,80,82}\text{Kr}(^3\text{He},d)$ reactions. This work, combined with the results of previously published $^{84,86}\text{Kr}(^3\text{He},d)$ measurements,^{1,2} yields information on the systematic trends in the distribution of proton strength between ^{79}Rb and ^{87}Rb . A preliminary analysis of the present work has been presented elsewhere.^{3,4}

EXPERIMENTAL PROCEDURE

Beams of 18-MeV ^3He ions were provided by the University of Pennsylvania Tandem Van de Graaff accelerator. Isotopically-enriched samples of Kr gas were contained in a gas cell described in greater detail below. Isotopic composition of the gases used is listed in Table I. Outgoing deuterons were momentum analyzed in a multi-angle magnetic spectrograph and detected using Ilford K2 nuclear emulsion plates. Spectra were recorded in steps of 7.5° (lab) except for the $^{78}\text{Kr}(^3\text{He},d)$ reaction for which a separate exposure at intermediate angles was

performed.

The older ($^3\text{He},d$) experiments^{1,2} used a recirculating gas system including a gas cell with no entrance window.⁵ That apparatus was unsuitable for the present work because the large amounts of gas required to fill the recirculating system would have made it impossible to use the expensive lighter isotopes of krypton. As a result, the cell was redesigned to permit a thin nickel window across the entrance snout. In addition, the gas handling system was redesigned to reduce its volume as much as possible. The entrance window was $64\ \mu\text{m}$ thick Ni, corresponding to an areal density of about $550\ \mu\text{g}/\text{cm}^2$. Reaction products exited through a $415\ \mu\text{g}/\text{cm}^2$ Mylar window. With the new design, the dominant contributions to the energy resolution are the straggling of the beam in the entrance window and the energy loss of the beam in the target gas. The experimental energy resolution was roughly 50 keV full width at half maximum (FWHM). One major advantage of a gas cell is that the target thickness can be calculated from the gas pressure which is accurately measured. It is estimated that absolute cross-section measurements presented herein are accurate to within 5–10%.

EXPERIMENTAL RESULTS

Typical spectra from the $^{78,80,82}\text{Kr}(^3\text{He},d)^{79,81,83}\text{Rb}$ reactions are shown in Figs. 1–3. Peak centroids and sums were obtained using the peak-fitting program AUTOFIT,⁶ and were used to calculate excitation energies and angular distributions.

A special fitting program was used to fine tune the spectrograph energy calibration using peaks of known excitation energy in the spectrum. In the process of this fit-

TABLE I. Composition of gases used in the present experiments.

Target	Composition (%)					
	78	80	82	83	84	86
^{78}Kr	99.5	0.5				
^{80}Kr	4.8	91.8	3.4			
^{82}Kr		1.8	92.1	5.9	0.2	
^{84}Kr			0.8	5.6	90.4	3.2
^{86}Kr					0.4	99.6

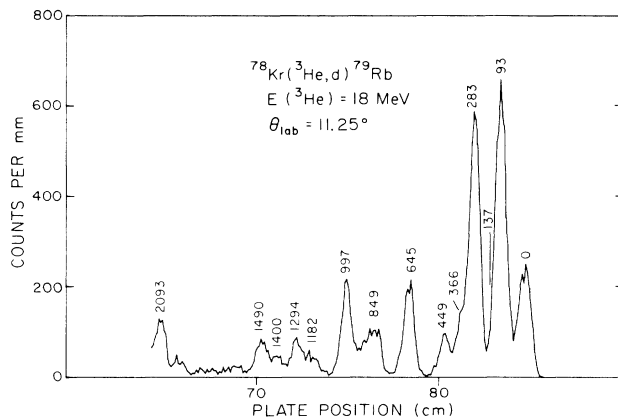


FIG. 1. Typical spectrum for the reaction $^{78}\text{Kr}(^3\text{He},d)^{79}\text{Rb}$.

ting, it was discovered that the positions of the ground-state peaks for the $^{78,82}\text{Kr}(^3\text{He},d)$ reactions deviated from those predicted using the tabulated masses of the constituents⁷ and the calculated energy loss of the beam in the entrance window and target gas. Since small peaks arising from impurity contributions of other Kr isotopes were present in each spectrum, it was possible to verify that this discrepancy was due to an actual deviation from the calculated Q value and not some difference in the spectrograph settings between experiments. The relative positions of the $\text{Kr}(^3\text{He},d)$ peaks can be used to calculate the Q values of the $^{78,82}\text{Kr}(^3\text{He},d)$ reactions, assuming that the other $\text{Kr}(^3\text{He},d)$ Q values are exactly those given by the mass tables. The resulting experimental Q values (all in MeV) are: $^{78}\text{Kr}(^3\text{He},d)^{79}\text{Rb}$, $Q = -1.585$; $^{80}\text{Kr}(^3\text{He},d)^{81}\text{Rb}$, $Q = -0.637$; $^{82}\text{Kr}(^3\text{He},d)^{83}\text{Rb}$, $Q = +0.288$, all \pm about 10 keV. These are to be compared with values in Ref. 7 of -1.518 ± 0.028 , -0.636 ± 0.023 , and $+0.247 \pm 0.021$. Differences are thus 66 and 41 keV for ^{78}Kr and ^{82}Kr , respectively—or roughly twice the quoted uncertainties of Ref. 7.

Angular distributions of the states observed are shown in Figs. 4–11, along with the distorted-wave Born ap-

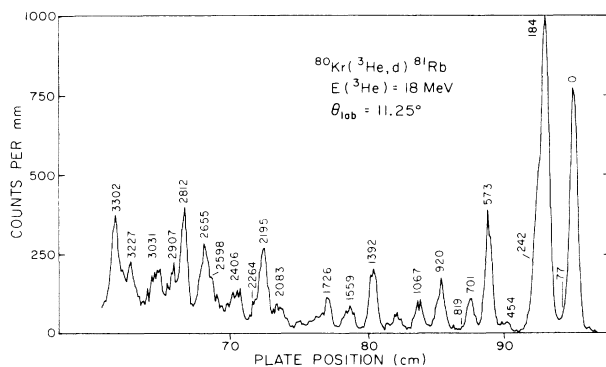


FIG. 2. Typical spectrum for the reaction $^{80}\text{Kr}(^3\text{He},d)^{81}\text{Rb}$.

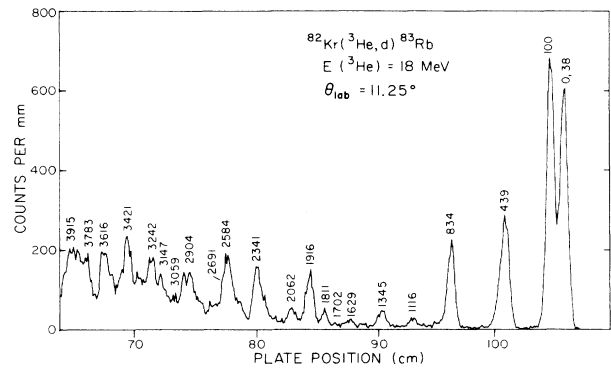


FIG. 3. Typical spectrum for the reaction $^{82}\text{Kr}(^3\text{He},d)^{83}\text{Rb}$.

proximation (DWBA) fits obtained. Because of the relatively poor energy resolution and the higher density of states in the lighter Rb isotopes, many of the angular distributions are characteristic of a sum of l values and are assumed to be unresolved doublets. Because of the large difference in shape between the DWBA curves for different l values, spectroscopic factors for the different contributions could be reliably extracted. Normalizations of the theoretical curves to the data were calculated using a

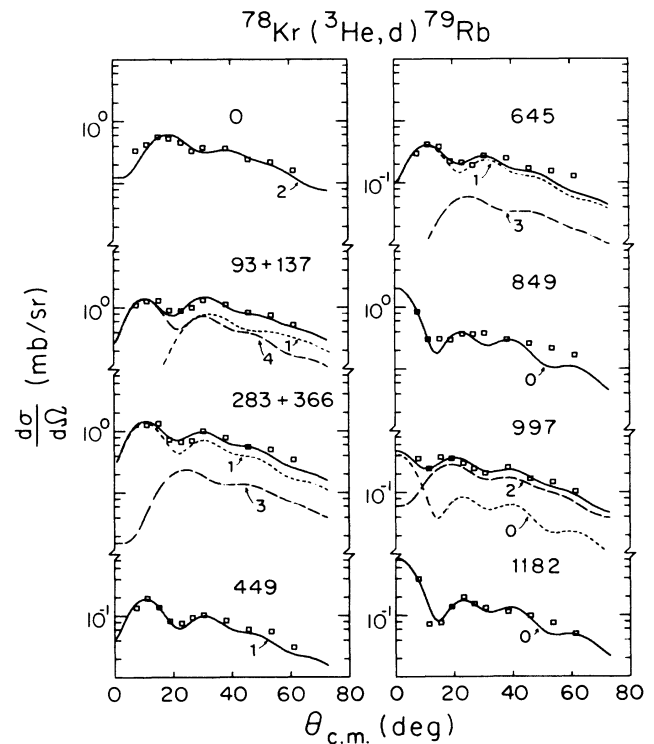


FIG. 4. Angular distributions for states populated in the $^{78}\text{Kr}(^3\text{He},d)^{79}\text{Rb}$ reaction. Excitation energies are given in keV. DWBA curves are labeled by l value. Where several l values are present, the solid curve is the sum.

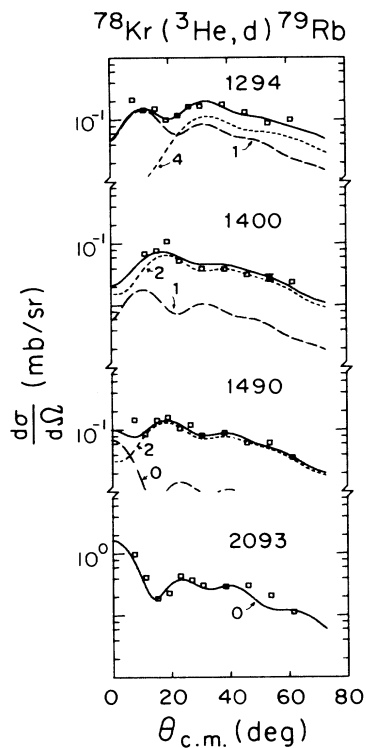


FIG. 5. Additional angular distributions for states populated in the $^{78}\text{Kr}(^3\text{He},d)^{79}\text{Rb}$ reaction. Excitation energies are given in keV. DWBA curves are labeled by l value. Where several l values are present, the solid curve is the sum.

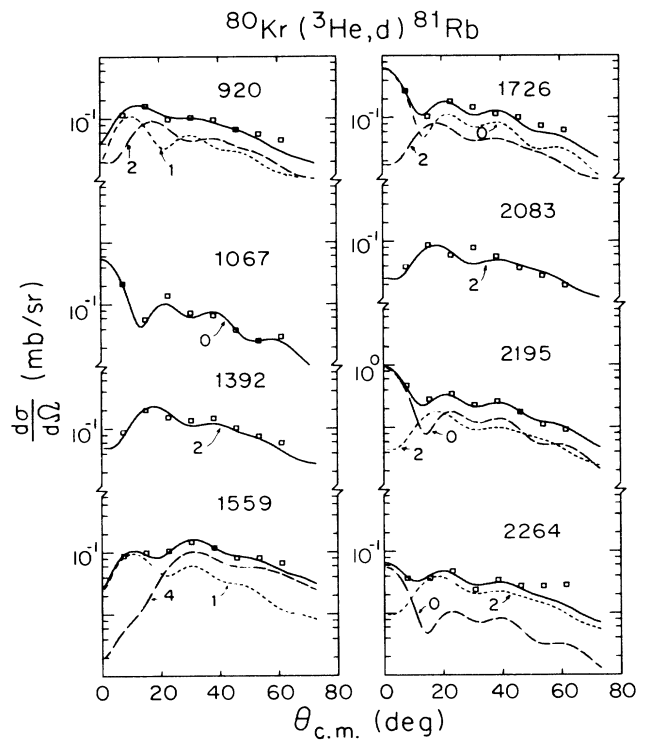


FIG. 7. Additional angular distributions for states populated in the $^{80}\text{Kr}(^3\text{He},d)^{81}\text{Rb}$ reaction. Excitation energies are given in keV. DWBA curves are labeled by l value. Where several l values are present, the solid curve is the sum.

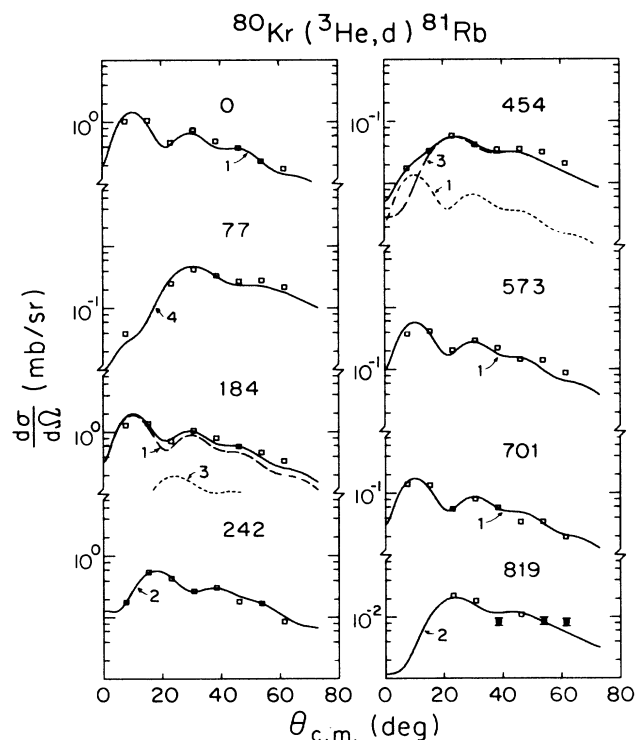


FIG. 6. Angular distributions for states populated in the $^{80}\text{Kr}(^3\text{He},d)^{81}\text{Rb}$ reaction. Excitation energies are given in keV. DWBA curves are labeled by l value. Where several l values are present, the solid curve is the sum.

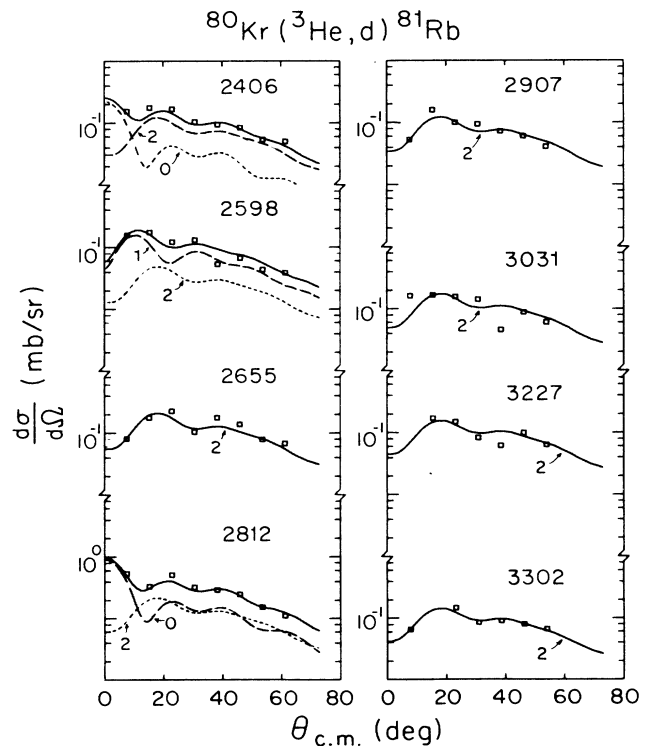


FIG. 8. Further angular distributions for states populated in the $^{80}\text{Kr}(^3\text{He},d)^{81}\text{Rb}$ reaction. Excitation energies are given in keV. DWBA curves are labeled by l value. Where several l values are present, the solid curve is the sum.

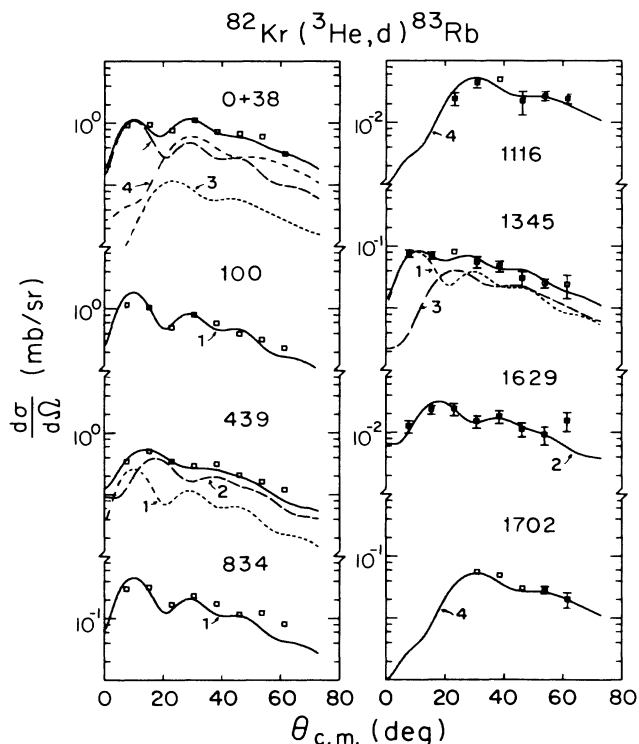


FIG. 9. Angular distributions for states populated in the $^{82}\text{Kr}(^3\text{He},d)^{83}\text{Rb}$ reaction. Excitation energies are given in keV. DWBA curves are labeled by l value. Where several l values are present, the solid curve is the sum.

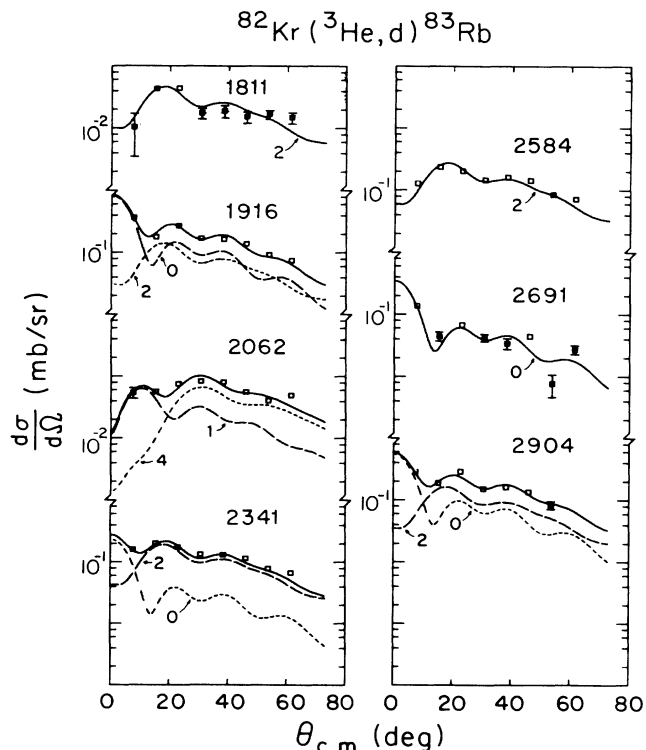


FIG. 10. Additional angular distributions for states populated in the $^{82}\text{Kr}(^3\text{He},d)^{83}\text{Rb}$ reaction. Excitation energies are given in keV. DWBA curves are labeled by l value. Where several l values are present, the solid curve is the sum.

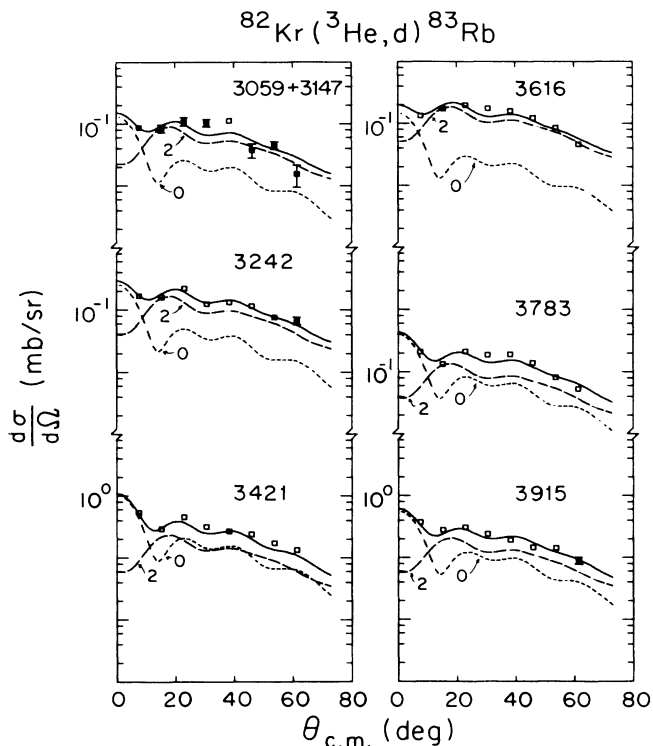


FIG. 11. Further angular distributions for states populated in the $^{82}\text{Kr}(^3\text{He},d)^{83}\text{Rb}$ reaction. Excitation energies are given in keV. DWBA curves are labeled by l value. Where several l values are present, the solid curve is the sum.

chi-squared fitting procedure. The theoretical fits are the result of zero-range DWBA calculations using the computer code DWUCK⁸ and the optical-model parameters listed in Table II. The spectroscopic strengths were calculated using the formula $G_{lj} = (2j + 1)R / 4.42$, where R is the ratio of experimental to theoretical cross sections. Spectroscopic factors, S_{lj} , were calculated using $G_{lj} = (2j + 1)C^2 S_{lj}$, where C^2 is the square of the isospin Clebsch-Gordan coefficient for the transfer. The assumption is made that all states observed have total isospin T equal to its minimum possible value $(N - Z) / 2$. The square of the Clebsch-Gordan coefficient ranges from 0.933 for proton transfer onto ^{86}Kr to 0.857 for transfer onto ^{78}Kr . In calculating G_{lj} and S_{lj} a knowledge of j is required but the angular distributions depend only on the transferred l . For many low-lying states, other information exists which determines j uniquely. All states for which no such information exists were assumed to be $2p_{1/2}$, $2d_{5/2}$, $1f_{5/2}$, and $1g_{9/2}$ for $l = 1, 2, 3$, and 4 , respectively. In the case of ^{79}Rb , the lowest $l = 1$ transfer was assumed to be $2p_{3/2}$ despite the lack of any other information because this is the case in all other isotopes.

One test of the accuracy of the absolute cross-section magnitude is the sum of the spectroscopic strengths. The ideal situation would be the observation of all of the transfer strength to an orbital which was initially empty, but this situation is rarely realized. However, it is sometimes possible to use the sum of G_{lj} for several orbitals as a test, since the sum of strength over all orbitals available

TABLE II. Optical-model parameters used in the present DWBA analysis. Strengths in MeV; lengths in fm.

	V	r	a	W	W'	r'	a'	V_{ls}	r	a	r_c
^3He	170	1.14	0.74	20		1.60	0.80				1.40
d	98	1.10	0.85		72	1.40	0.70	6	1.10	0.85	1.30
p	a	1.20	0.65					$\lambda=25$			1.20

^aAdjusted to fit correct proton separation energy.

should equal the number of vacancies, regardless of how the vacancies are distributed among the orbitals. In the present case, there are 14 proton holes to distribute among the $2p_{3/2}$, $1f_{5/2}$, $2p_{1/2}$, and $1g_{9/2}$ orbitals which fill the $Z=50$ shell. The sum-rule limit for G_{ij} (Ref. 9) is thus 14 minus $1/(N-Z+1)$ times the number of neutron

holes in the $N=50$ shell. This limit ranges from 12.86 for ^{78}Kr to 14 for ^{86}Kr which has a closed $N=50$ shell. Table VIII (discussed in more detail later) shows that within the 20% uncertainty usually associated with spectroscopic strengths there is no evidence for a discrepancy from this simple shell-model prediction.

TABLE III. Results of the $^{78}\text{Kr}(^3\text{He,d})^{79}\text{Rb}$ reaction. See text for discussion of calculation of G_{ij} .

E_x (keV)	1	J^π	G_{ij}	Compilation ^a	
				E_x (keV)	J^π
0	2	$\frac{5}{2}^+$	0.73	0	$\frac{5}{2}^+$
				39	$(\frac{3}{2}, \frac{5}{2})$
				47	$(\frac{7}{2}^+)$
93	4	$\frac{9}{2}^+$	9.12	97	$(\frac{9}{2}^+)$
137	1	$(\frac{1}{2}, \frac{3}{2})^-$	0.90	144	$(\frac{1}{2}^+, \frac{3}{2}, \frac{5}{2})$
				174	$(\frac{5}{2}^-)$
283	1	$(\frac{1}{2}, \frac{3}{2})^-$	1.09	285	$(\frac{1}{2}, \frac{3}{2}, \frac{5}{2})$
366	3	$(\frac{5}{2}, \frac{7}{2})^-$	2.25	357	$(\frac{1}{2}, \frac{3}{2}, \frac{5}{2})$
				363	$(\frac{1}{2}, \frac{3}{2}, \frac{5}{2})$
449	1	$(\frac{1}{2}, \frac{3}{2})^-$	0.15	452	$(\frac{1}{2}, \frac{3}{2}, \frac{5}{2})$
				594	$(\frac{11}{2}^+)$
				598	$(\frac{13}{2}^+)$
				651	$(\frac{1}{2}, \frac{3}{2}, \frac{5}{2})$
645	3	$(\frac{5}{2}, \frac{7}{2})^-$	0.53	680	$(\frac{9}{2}^-)$
				849	$\frac{1}{2}^+$
				997	$\frac{1}{2}^+$
1182	0	$\frac{1}{2}^+$	0.085	1349	$(\frac{13}{2}^-)$
					1294
1294	1	$(\frac{1}{2}, \frac{3}{2})^-$	0.091	1353	$(\frac{17}{2}^+)$
				4	$(\frac{7}{2}, \frac{9}{2})^+$
1400	1	$(\frac{1}{2}, \frac{3}{2})^-$	0.029	1404	$(\frac{15}{2}^+)$
				2	$(\frac{3}{2}, \frac{5}{2})^+$
1490	0	$\frac{1}{2}^+$	0.0068	2164	$(\frac{17}{2}^-)$
					2
2093	0	$\frac{1}{2}^+$	0.16		

^aReference 21.

TABLE IV. Results of the $^{80}\text{Kr}(^3\text{He,d})^{81}\text{Rb}$ reaction. See text for discussion of calculation of G_{ij} . The compilation includes the results of the present work.

E_x (keV)	1	J^π	G_{ij}	Compilation ^a	
				E_x (keV)	J^π
0	1	$\frac{3}{2}^-$	1.13	0	$\frac{3}{2}^-$
77	4	$\frac{9}{2}^+$	6.22	86	$\frac{9}{2}^+$
184	3	$\frac{5}{2}^-$	2.14	153	$(\frac{5}{2})^-$
	1	$(\frac{1}{2}, \frac{3}{2})^-$	1.71	188	$(\frac{1}{2}^-, \frac{3}{2}^-)$
242	2	$(\frac{3}{2}, \frac{5}{2})^+$	0.75	245	$(\frac{5}{2})^+$
				301	$(\frac{3}{2})^-$
				434	$(\frac{5}{2}^+, \frac{7}{2}, \frac{9}{2}^+)$
454	3	$(\frac{5}{2}, \frac{7}{2})^-$	0.58	443	$(\frac{1}{2}, \frac{3}{2})$
	1	$(\frac{1}{2}, \frac{3}{2})^-$	0.011	454	$(\frac{5}{2})^-$
				463	$(\frac{1}{2}^+, \frac{3}{2}, \frac{5}{2}^+)$
				487	
				497	
573	1	$(\frac{1}{2}, \frac{3}{2})^-$	0.47	575	$(\frac{1}{2})^-$
				612	
				631	$\frac{5}{2}^+, \frac{7}{2}^-$
701	1	$(\frac{1}{2}, \frac{3}{2})^-$	0.14	702	$(\frac{1}{2}, \frac{3}{2}, \frac{5}{2}^+)$
				709	
				712	$(\frac{1}{2}, \frac{3}{2})$
819	2	$(\frac{3}{2}, \frac{5}{2})^+$	0.20	828	$(\frac{5}{2})^+$
920	2	$(\frac{3}{2}, \frac{5}{2})^+$	0.10	909	$(\frac{1}{2}^+, \frac{3}{2})$
	1	$(\frac{1}{2}, \frac{3}{2})^-$	0.083	913	
				923	$(\frac{1}{2}, \frac{3}{2})$
				987	
				1035	
1067	0	$\frac{1}{2}^+$	0.056	1062	$\frac{1}{2}^+$
				1175	
				1219	$(\frac{1}{2}^+, \frac{3}{2})$
				1243	$(\frac{1}{2}^+, \frac{3}{2})$
				1305	$(\frac{7}{2}, \frac{9}{2}^+)$
1392	2	$(\frac{3}{2}, \frac{5}{2})^+$	0.24	1382	$(\frac{3}{2})^-$
				1416	
				1464	
				1513	$(\frac{1}{2}, \frac{3}{2})$
1559	4	$(\frac{7}{2}, \frac{9}{2})^+$	1.05	1554	$(\frac{1}{2}^-, \frac{3}{2}^-)$
	1	$(\frac{1}{2}, \frac{3}{2})^-$	0.068	1584	
				1739	
1726	0	$\frac{1}{2}^+$	0.057	1774	
	2	$(\frac{3}{2}, \frac{5}{2})^+$	0.079	1804	$(\frac{1}{2}, \frac{3}{2})$
				1848	$(\frac{1}{2}^+, \frac{3}{2})$
				1920	
2083	2	$(\frac{3}{2}, \frac{5}{2})^+$	0.086	2072	$(\frac{5}{2})^+$
2195	0	$\frac{1}{2}^+$	0.080	2165	$(\frac{1}{2}^+, \frac{3}{2})$

TABLE IV. (Continued).

E_x (keV)	1	J^π	G_{ij}	Compilation ^a	
				E_x (keV)	J^π
2195	2	$(\frac{3}{2}, \frac{5}{2})^+$	0.17	2200	$(\frac{5}{2}^+)$
2264	0	$\frac{1}{2}^+$	0.0050	2264	
	2	$(\frac{3}{2}, \frac{5}{2})^+$	0.035	2295	
2406	0	$\frac{1}{2}^+$	0.020	2400	$(\frac{5}{2}^+)$
	2	$(\frac{3}{2}, \frac{5}{2})^+$	0.11		
2598	1	$(\frac{1}{2}, \frac{3}{2})^-$	0.095	2576	
	2	$(\frac{3}{2}, \frac{5}{2})^+$	0.045	2608	
2655	2	$(\frac{3}{2}, \frac{5}{2})^+$	0.19	2638	$\frac{3}{2}^+, \frac{5}{2}^+$
2812	0	$\frac{1}{2}^+$	0.085	2807	$(\frac{1}{2}^+)$
	2	$(\frac{3}{2}, \frac{5}{2})^+$	0.20		
2907	2	$(\frac{3}{2}, \frac{5}{2})^+$	0.11	2907	$\frac{3}{2}^+, \frac{5}{2}^+$
3031	2	$(\frac{3}{2}, \frac{5}{2})^+$	0.15	3031	$\frac{3}{2}^+, \frac{5}{2}^+$
3227	2	$(\frac{3}{2}, \frac{5}{2})^+$	0.13	3242	$(\frac{5}{2}^+)$
3302	2	$(\frac{3}{2}, \frac{5}{2})^+$	0.12	3295	
				3765	

^aReference 22.

The excitation energies and spectroscopic information for levels excited in the (³He,d) reaction on all five Kr isotopes are listed in Tables III–VII. In many cases, the peak-separation program was not capable of resolving two levels sufficiently to yield two complete angular distributions and the summed angular distribution is shown in the figures. Occasionally, however, a partial separation was sufficient to indicate which member of the doublet corresponded to a particular l value, and this fact is reflected in the numbers listed in the tables.

It is estimated that the absolute values of G_{ij} are correct to within about 15–20%. Additional uncertainty is involved in cases for which several curves must be added to fit a particular angular distribution. This procedure causes particular problems for $l=3$ and 4 mixtures into predominantly low- l states, because $l=3$ and 4 are kinematically suppressed, and a large spectroscopic strength can result in a relatively small experimental contribution to the angular distribution. The situation is unusually difficult in ⁸³Rb where the majority of the $2p_{3/2}$, $1f_{5/2}$, and $1g_{9/2}$ strengths occur in one partially resolved peak low in the spectrum. The use of a chi-squared fitting procedure reduces the uncertainty in extracting normalizations but an additional 5–10% is introduced. This problem may partially explain the anomalously large summed strength seen for ⁸³Rb.

The spectroscopic information extracted for proton transfer on all even- A Kr targets is illustrated in Figs. 12 and 13 and summed spectroscopic strengths are listed in Table VIII. The figures show S_{ij} to facilitate plotting several l values on the same scale. The levels divide naturally into two groups, most of the $l=1, 3,$ and 4 strength occurring low in energy while $l=0$ and 2 dom-

inate the higher excitation energies. Several systematic trends are immediately apparent. The low-energy region is dominated by four strong states with $J^\pi = \frac{1}{2}^-, \frac{3}{2}^-, \frac{5}{2}^-$, and $\frac{9}{2}^+$. Moving away from the closed neutron shell at ⁸⁷Rb, these strong single-particle states move to lower excitation energy and the total strength becomes spread among several states. The distribution of the $l=0$ and 2 states is somewhat more complex. The spectroscopic strength in these cases is much more fractioned even at the closed shell. This spreading is presumably due to the fact that the $2d_{5/2}$ and $3s_{1/2}$ single-particle levels are very high in energy and thus there are a large number of core-excited configurations with which they can mix. As with the lower levels, the centroids of the $l=0$ and 2 strengths move down in energy with decreasing A . One outstanding feature of the $2d_{5/2}$ distribution is the presence of one strong low-lying state that drops in energy somewhat faster than the remaining levels. Although this state is relatively strong compared to the other $l=2$ transfers, it still represents less than 20% of the total $2d_{5/2}$ strength. This low-lying $\frac{5}{2}^+$ level actually becomes the ground state in ⁷⁹Rb.

Several systematic trends are also evident in Table VIII. With the exception of ⁷⁹Rb, all nuclei contain roughly 25% more $2p_{1/2}$ spectroscopic strength than allowed by the sum rule. This surplus is partially the result of assuming that all states populated by $l=1$ transfer are $2p_{1/2}$ unless other information exists to determine j uniquely. It may also be due to the use of too large a value for the bound-state spin-orbit strength, as decreasing this parameter increases the $j_<$ theoretical cross sections, without much change for $j_>$. The $1g_{9/2}$ summed strength also occasionally exceeds the maximum allowed

TABLE V. Results of the $^{82}\text{Kr}(^3\text{He},d)^{83}\text{Rb}$ reaction. See text for discussion of calculation of G_{lj} . Calculated values are from Ref. 12. Previous work includes compiled results (Ref. 23) and recent (HI,xn γ) experiment (Ref. 24). Levels unique to Ref. 24 are marked with an asterisk.

Experimental				Calculated			Previous work	
E_x (keV)	1	J^π	G_{lj}	E_x (keV)	J^π	G_{lj}	E_x (keV)	J^π
4	3	$\frac{5}{2}^-$	2.02	0	$\frac{5}{2}^-$	1.06	0	$\frac{5}{2}^-$
	1	$\frac{3}{2}^-$	0.99	10	$\frac{3}{2}^-$	0.70	5	$\frac{3}{2}^-$
38	4	$\frac{9}{2}^+$	9.12	44	$\frac{9}{2}^+$	7.74	42	$\frac{9}{2}^+$
100	1	$(\frac{1}{2}, \frac{3}{2})^-$	1.90	100	$\frac{1}{2}^-$	1.21	100	$(\frac{1}{2}, \frac{3}{2})^-$
							390	$(\frac{3}{2})^-$
439	1	$(\frac{1}{2}, \frac{3}{2})^-$	0.25	478	$\frac{5}{2}^+$		424	$\frac{5}{2}^+$
	2	$(\frac{3}{2}, \frac{5}{2})^+$	0.56				565	
				683	$\frac{1}{2}^-$	0.10		
				700	$\frac{3}{2}^-$	0.02		
				748	$\frac{5}{2}^-$	0.04	737	$\frac{7}{2}^-$
				797	$\frac{3}{2}^-$	0.07	794*	$\frac{13}{2}^+$
834	1	$(\frac{1}{2}, \frac{3}{2})^-$	0.42	810	$\frac{1}{2}^-$	0.63	805	$\frac{7}{2}^+$
				821	$\frac{5}{2}^-$	0.07		
				929	$\frac{3}{2}^-$	0.02		
				1005	$\frac{5}{2}^-$	0.02		
							1037	$\frac{11}{2}^+$
			1044					
			1055					
			1083					
			1086					
1116	4	$(\frac{7}{2}, \frac{9}{2})^+$	0.68				1097*	
							1103	$\frac{9}{2}^-$
							1202	
							1243	
1345	3	$(\frac{5}{2}, \frac{7}{2})^-$	0.44					
	1	$(\frac{1}{2}, \frac{3}{2})^-$	0.064				1587*	$(\frac{9}{2}, \frac{13}{2})$
1629	2	$(\frac{3}{2}, \frac{5}{2})^+$	0.035					
1702	4	$(\frac{7}{2}, \frac{9}{2})^+$	0.68				1696	
							1749	$\frac{11}{2}^-$
							1781*	
							1799	$(\frac{5}{2}, \frac{9}{2})$
							1809	
1811	2	$(\frac{3}{2}, \frac{5}{2})^+$	0.053				1890*	$\frac{17}{2}^+$
							1917	
1916	0	$\frac{1}{2}^+$	0.085					
	2	$(\frac{3}{2}, \frac{5}{2})^+$	0.16				1943*	$\frac{15}{2}^+$
							1952	
							2020	
							2056	
2062	4	$(\frac{7}{2}, \frac{9}{2})^+$	0.74					

TABLE V. (Continued).

Experimental				Calculated			Previous work	
E_x (keV)	1	J^π	G_{lj}	E_x (keV)	J^π	G_{lj}	E_x (keV)	J^π
2062	1	$(\frac{1}{2}, \frac{3}{2})^-$	0.046				2074*	$(\frac{13}{2})$
							2091	
							2102*	$\frac{13}{2}$
							2134	$(\frac{5}{2}, \frac{7}{2})^+$
							2147	$(\frac{5}{2}, \frac{7}{2})^+$
							2178	$(\frac{5}{2} - \frac{9}{2})^+$
							2207*	$(\frac{11}{2}, \frac{13}{2})$
							2310*	
							2314*	$(\frac{13}{2}^-)$
							2319*	
2341	0	$\frac{1}{2}^+$	0.022				2414*	$(\frac{15}{2}^-)$
							2577*	$(\frac{15}{2})$
2584	2	$(\frac{3}{2}, \frac{5}{2})^+$	0.27				2597*	$(\frac{17}{2}^-)$
2691	0	$\frac{1}{2}^+$	0.035				2700*	$(\frac{17}{2})$
							2733	$(\frac{13}{2}, \frac{17}{2})$
2904	0	$\frac{1}{2}^+$	0.049				2860*	
							2	$(\frac{3}{2}, \frac{5}{2})^+$
3059	0	$\frac{1}{2}^+$	0.012				2959*	$(\frac{19}{2})$
3147	2	$(\frac{3}{2}, \frac{5}{2})^+$	0.081					
3242	0	$\frac{1}{2}^+$	0.023					
3421	0	$\frac{1}{2}^+$	0.091				3369*	$(\frac{21}{2})$
							2	$(\frac{3}{2}, \frac{5}{2})^+$
3616	0	$\frac{1}{2}^+$	0.013				3560*	
							2	$(\frac{3}{2}, \frac{5}{2})^+$
3783	0	$\frac{1}{2}^+$	0.035				3728*	
							2	$(\frac{3}{2}, \frac{5}{2})^+$
3915	0	$\frac{1}{2}^+$	0.049					
							2	$(\frac{3}{2}, \frac{5}{2})^+$

but not by a significant amount. The drop in the excitation energy of the $2p_{1/2}$ and $1g_{9/2}$ levels seen in the figures shows up clearly in the weighted energies of these states. This drop seems to occur mostly between ^{87}Rb and ^{83}Rb . The $2p_{3/2}$ and $1f_{5/2}$ strengths are concentrated in fewer states and thus the weighted energy moves around

with the energy of the dominant state. No clear trends are apparent in the latter numbers.

The summed spectroscopic strengths show trends that are less readily apparent in the figures. Despite the fact that, for experimental reasons, a progressively smaller range of excitation energy was investigated, the amount of

TABLE VI. Results of the $^{84}\text{Kr}(^3\text{He,d})^{85}\text{Rb}$ reaction (Ref. 1). See text for discussion of calculation of G_{ij} . Calculated values are from Ref. 12.

E_x (keV)	Experimental			E_x (keV)	Calculated	
	1	J^π	G_{ij}		J^π	G_{ij}
0	3	$\frac{5}{2}^-$	1.78	0	$\frac{5}{2}^-$	1.57
151	1	$\frac{3}{2}^-$	0.82	160	$\frac{3}{2}^-$	0.98
281	1	$\frac{1}{2}^-$	1.53	270	$\frac{1}{2}^-$	1.12
514	4	$\frac{9}{2}^+$	6.84	520	$\frac{9}{2}^+$	5.84
735	1	$(\frac{1}{2}, \frac{3}{2})^-$	0.087	850	$\frac{3}{2}^-$	0.05
883	(1)	$(\frac{1}{2}, \frac{3}{2})^-$	0.14	890	$\frac{1}{2}^-$	0.32
950	2	$(\frac{3}{2}, \frac{5}{2})^+$	0.35	810	$\frac{5}{2}^+$	0.75
				900	$\frac{5}{2}^-$	0.12
				1100	$\frac{5}{2}^-$	0.07
1175	4	$(\frac{7}{2}, \frac{9}{2})^+$	0.26			
1294	1	$(\frac{1}{2}, \frac{3}{2})^-$	0.18	1110	$\frac{1}{2}^-$	0.51
				1120	$\frac{3}{2}^-$	0.13
				1220	$\frac{3}{2}^-$	0.03
				1440	$\frac{5}{2}^-$	0.03
1789	1	$(\frac{1}{2}, \frac{3}{2})^-$	0.046			
1954	1	$(\frac{1}{2}, \frac{3}{2})^-$	0.027			
2050	4	$(\frac{7}{2}, \frac{9}{2})^+$	1.05	1680	$\frac{9}{2}^+$	2.10
2375	1	$(\frac{1}{2}, \frac{3}{2})^-$	0.039			
2514	4	$(\frac{7}{2}, \frac{9}{2})^+$	0.46	2550	$\frac{9}{2}^+$	0.29
2602	1	$(\frac{1}{2}, \frac{3}{2})^-$	0.019	2580	$\frac{1}{2}^-$	0.01
2730	2	$(\frac{3}{2}, \frac{5}{2})^+$	0.038	2870	$\frac{5}{2}^+$	0.19
2801	0	$\frac{1}{2}^+$	0.0072			
2948	0	$\frac{1}{2}^+$	0.015			
3024	2	$(\frac{3}{2}, \frac{5}{2})^+$	0.13			
3148	2	$(\frac{3}{2}, \frac{5}{2})^+$	0.16			
3200	2	$(\frac{3}{2}, \frac{5}{2})^+$	0.18			
3310	(1)	$(\frac{1}{2}, \frac{3}{2})^-$	0.023			
3398	1	$(\frac{1}{2}, \frac{3}{2})^-$	0.027			
3541	2	$(\frac{3}{2}, \frac{5}{2})^+$	0.089			
3598	2	$(\frac{3}{2}, \frac{5}{2})^+$	0.14			
3656	0	$\frac{1}{2}^+$	0.048			
	2	$(\frac{3}{2}, \frac{5}{2})^+$	0.039			
3698	0	$\frac{1}{2}^+$	0.10			
3886	2	$(\frac{3}{2}, \frac{5}{2})^+$	0.047			
3981	0	$\frac{1}{2}^+$	0.046			
4039	2	$(\frac{3}{2}, \frac{5}{2})^+$	0.16			
4117	2	$(\frac{3}{2}, \frac{5}{2})^+$	0.15			
4154	(2)	$(\frac{3}{2}, \frac{5}{2})^+$	0.059			
4220	(0)	$(\frac{1}{2})^+$	0.019			

TABLE VI. (Continued).

E_x (keV)	Experimental			Calculated		
	1	J^π	G_{ij}	E_x (keV)	J^π	G_{ij}
4343	2	$(\frac{3}{2}, \frac{5}{2})^+$	0.064			
4484	2	$(\frac{3}{2}, \frac{5}{2})^+$	0.029			
4575	2	$(\frac{3}{2}, \frac{5}{2})^+$	0.082			
4631	0	$\frac{1}{2}^+$	0.011			
4729	1	$(\frac{1}{2}, \frac{3}{2})^-$	0.082			
4756	2	$(\frac{3}{2}, \frac{5}{2})^+$	0.089			
4861	2	$(\frac{3}{2}, \frac{5}{2})^+$	0.096			
4913	0	$\frac{1}{2}^+$	0.052			
5013	2	$(\frac{3}{2}, \frac{5}{2})^+$	0.058			
5074	2	$(\frac{3}{2}, \frac{5}{2})^+$	0.050			
5127	2	$(\frac{3}{2}, \frac{5}{2})^+$	0.042			
5186	0	$\frac{1}{2}^+$	0.012			
5245	2	$(\frac{3}{2}, \frac{5}{2})^+$	0.065			
5367	(2)	$(\frac{3}{2}, \frac{5}{2})^+$	0.063			
5444	2	$(\frac{3}{2}, \frac{5}{2})^+$	0.039			
5516	0	$\frac{1}{2}^+$	0.034			
5563	(2)	$(\frac{3}{2}, \frac{5}{2})^+$	0.039			
5643	(2)	$(\frac{3}{2}, \frac{5}{2})^+$	0.029			
5668	2	$(\frac{3}{2}, \frac{5}{2})^+$	0.029			
5719	(1)	$(\frac{1}{2}, \frac{3}{2})^-$	0.048			
5815	(2)	$(\frac{3}{2}, \frac{5}{2})^+$	0.039			
5996	(2)	$(\frac{3}{2}, \frac{5}{2})^+$	0.067			
6065	0	$\frac{1}{2}^+$	0.034			
6185	2	$(\frac{3}{2}, \frac{5}{2})^+$	0.036			

$l=0$ strength observed is roughly constant. The situation is similar for $l=2$ with the dramatic exception of ^{79}Rb , for which there seems to be considerably less $l=2$ strength present. However, problems with background and impurities which hindered extraction of states above 2.1 MeV in ^{79}Rb may have hidden some $l=2$ strength. These experimental difficulties should not have affected the amount of $l=1$ strength present since most of it occurs at lower excitation energy, but a significant deficit for this l value also occurs at ^{79}Rb . As discussed above, the extraction of $l=3$ and 4 strengths was hampered by the fact that some of the strength occurs in doublets. This additional uncertainty probably accounts for most of the fluctuation in the $1g_{9/2}$ strength but can not explain the steady rise in $1f_{5/2}$ strength.

COMPARISON TO THEORY

Two separate approaches have been used recently to theoretically calculate the occupancy of proton orbitals in

the Kr isotopes. One involved solving the BCS Hamiltonian for the ground state of ^{86}Kr .¹⁰ The prediction was that the $2p_{1/2}$ and $1g_{9/2}$ orbitals are almost totally empty while both the $2p_{3/2}$ and $1f_{5/2}$ orbitals are partially full. The theoretical values for summed strengths of 1.86, 1.01, 1.67, and 9.45 for $1f_{5/2}$, $2p_{3/2}$, $2p_{1/2}$, and $1g_{9/2}$, respectively, compare reasonably with the experimental results of 1.18, 1.36, 2.41, and 10.26, although the $1f_{5/2}$ orbital is not as empty as predicted by the theory.

A somewhat more ambitious calculation used spectral distribution methods and the Kuo effective interaction to derive ground-state proton occupancies for a large number of f - p shell nuclei including Kr.¹¹ Figure 1 in that article displayed these occupancies for all Kr isotopes between $A=76$ and 84. The prediction that the $1g_{9/2}$ orbital is almost empty for all of these nuclei is supported by our experiments. The $1f_{5/2}$ occupancy was predicted to fall smoothly with decreasing A from almost 4 particles to slightly more than 2, implying a steady rise in $l=3$ summed strength. Such an increase is seen in our data al-

though the experimental magnitude of the change is only about $\frac{2}{3}$ of the theoretical value. Substantial deviations were found, however, between the calculated and measured numbers for $l=1$ transfer. The $2p_{1/2}$ orbital was predicted to range from approximately half full at $N=48$ to almost totally full in the lighter isotopes. Although there is some difficulty in assigning j for some of the higher-energy levels, most of these nuclei have a low-lying state known to be $\frac{1}{2}^-$ from other work. In all cases, the strength present in that one state alone is much more than

predicted by this model. A similar rise in occupancy with decreasing A was indicated for the $2p_{3/2}$ orbital with values ranging from about 65% to about 90% full. This result also is in contradiction with experiment, especially for the lighter isotopes, where significantly more $2p_{3/2}$ strength is found than expected from this model.

Spectroscopic factors for individual states can be derived from the wave functions calculated for several odd- A Rb isotopes using core-particle coupling models. Recent published work includes studies of $^{83,85}\text{Rb}$ by

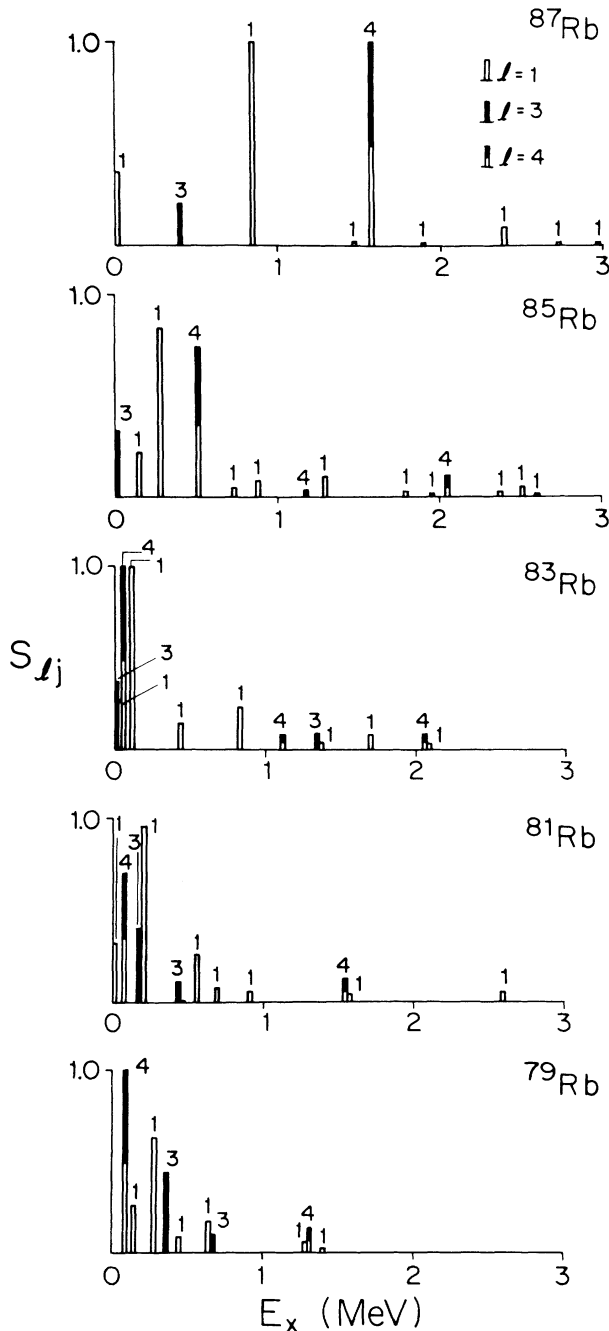


FIG. 12. Spectroscopic factors, S_{lj} , for levels populated with $l=1, 3,$ and 4 in the reactions $^{78,80,82,84,86}\text{Kr}(^3\text{He},d)^{79,81,83,85,87}\text{Rb}$.

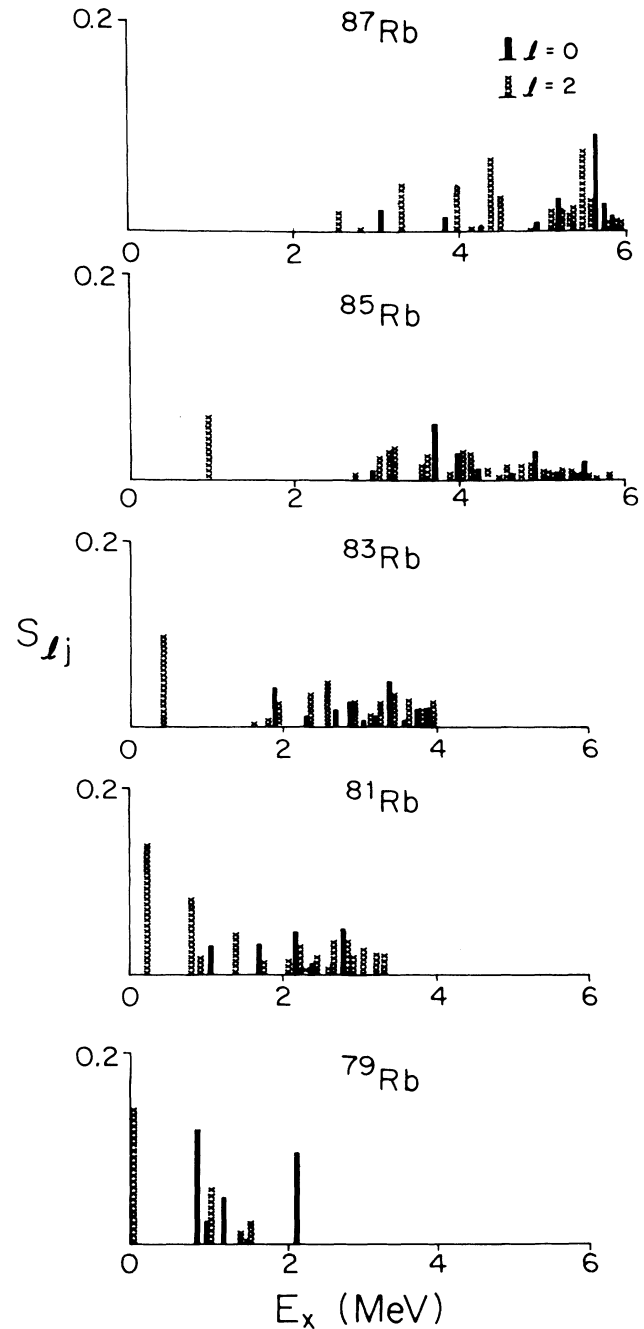


FIG. 13. Spectroscopic factors, S_{lj} , for levels populated with $l=0$ and 2 in the reactions $^{78,80,82,84,86}\text{Kr}(^3\text{He},d)^{79,81,83,85,87}\text{Rb}$.

TABLE VII. Results of the $^{86}\text{Kr}(^3\text{He,d})^{87}\text{Rb}$ reaction (Ref.2). See text for discussion of calculation of G_{ij} . Calculated values are from Ref. 13.

E_x (keV)	Experimental			E_x (keV)	Calculated	
	1	J^π	G_{ij}		J^π	G_{ij}
0	1	$\frac{3}{2}^-$	1.36	0	$\frac{3}{2}^-$	1.36
399	3	$\frac{5}{2}^-$	1.18	324	$\frac{5}{2}^-$	1.29
846	1	$(\frac{1}{2})^-$	2.04	830	$\frac{1}{2}^-$	1.33
1468	1	$(\frac{1}{2}, \frac{3}{2})^-$	0.031	1719	$\frac{3}{2}^-$	0.02
1578	4	$\frac{9}{2}^+$	9.87	1763	$\frac{9}{2}^+$	7.39
				1793	$\frac{5}{2}^-$	0.02
1893	1	$(\frac{1}{2}, \frac{3}{2})^-$	0.023	1851	$\frac{1}{2}^-$	0.17
				2053	$\frac{1}{2}^-$	0.41
				2130	$\frac{3}{2}^-$	0.02
				2345	$\frac{5}{2}^-$	0.04
2396	1	$(\frac{1}{2}, \frac{3}{2})^-$	0.17			
2548	2	$(\frac{3}{2}, \frac{5}{2})^+$	0.11			
2731	4	$(\frac{7}{2}, \frac{9}{2})^+$	0.14			
2810	2	$(\frac{3}{2}, \frac{5}{2})^+$	0.024			
2973	4	$(\frac{7}{2}, \frac{9}{2})^+$	0.13			
3060	0	$\frac{1}{2}^+$	0.036			
3309	2	$(\frac{3}{2}, \frac{5}{2})^+$	0.25			
3335	1	$(\frac{1}{2}, \frac{3}{2})^-$	0.058			
3692	1	$(\frac{1}{2}, \frac{3}{2})^-$	0.016			
	(4)	$(\frac{7}{2}, \frac{9}{2})^+$	0.12			
3764	1	$(\frac{1}{2}, \frac{3}{2})^-$	0.021			
3834	0	$\frac{1}{2}^+$	0.024			
3973	2	$(\frac{3}{2}, \frac{5}{2})^+$	0.24			
4146	2	$(\frac{3}{2}, \frac{5}{2})^+$	0.021			
4266	2	$(\frac{3}{2}, \frac{5}{2})^+$	0.031			
	(1)	$(\frac{1}{2}, \frac{3}{2})^-$	0.014			
4379	2	$(\frac{3}{2}, \frac{5}{2})^+$	0.39			
4492	2	$(\frac{3}{2}, \frac{5}{2})^+$	0.19			
4681	1	$(\frac{1}{2}, \frac{3}{2})^-$	0.034			
4862	0	$\frac{1}{2}^+$	0.003			
	2	$(\frac{3}{2}, \frac{5}{2})^+$	0.008			
4941	0	$\frac{1}{2}^+$	0.012			
5118	2	$(\frac{3}{2}, \frac{5}{2})^+$	0.12			
5196	0	$\frac{1}{2}^+$	0.056			
5233	2	$(\frac{3}{2}, \frac{5}{2})^+$	0.11			
5316	2	$(\frac{3}{2}, \frac{5}{2})^+$	0.089			
5347	2	$(\frac{3}{2}, \frac{5}{2})^+$	0.13			
5491	2	$(\frac{3}{2}, \frac{5}{2})^+$	0.43			

TABLE VII. (*Continued*).

E_x (keV)	Experimental		G_{ij}	E_x (keV)	Calculated	
	1	J^π			J^π	G_{ij}
5542	0	$\frac{1}{2}^+$	0.026			
	2	$(\frac{3}{2}, \frac{5}{2})^+$	0.17			
5634	0	$\frac{1}{2}^+$	0.17			
5750	0	$\frac{1}{2}^+$	0.044			
5802	0	$\frac{1}{2}^+$	0.016			
	2	$(\frac{3}{2}, \frac{5}{2})^+$	0.081			
5845	2	$(\frac{3}{2}, \frac{5}{2})^+$	0.056			
5884	2	$(\frac{3}{2}, \frac{5}{2})^+$	0.051			
5978	2	$(\frac{3}{2}, \frac{5}{2})^+$	0.13			
6018	0	$\frac{1}{2}^+$	0.076			
6089	2	$(\frac{3}{2}, \frac{5}{2})^+$	0.073			
6176	0	$\frac{1}{2}^+$	0.030			
6206	2	$(\frac{3}{2}, \frac{5}{2})^+$	0.071			
6307	2	$(\frac{3}{2}, \frac{5}{2})^+$	0.085			
6375	0	$\frac{1}{2}^+$	0.022			
	2	$(\frac{3}{2}, \frac{5}{2})^+$	0.083			
6468	0	$\frac{1}{2}^+$	0.034			
6512	2	$(\frac{3}{2}, \frac{5}{2})^+$	0.086			
6548	0	$\frac{1}{2}^+$	0.056			
6618	2	$(\frac{3}{2}, \frac{5}{2})^+$	0.092			
6652	2	$(\frac{3}{2}, \frac{5}{2})^+$	0.12			
6744	2	$(\frac{3}{2}, \frac{5}{2})^+$	0.10			
6791	0	$\frac{1}{2}^+$	0.022			
	2	$(\frac{3}{2}, \frac{5}{2})^+$	0.075			
6838	0	$\frac{1}{2}^+$	0.056			
6989	0	$\frac{1}{2}^+$	0.053			

Krishan, Basu, and Sen,¹² and ^{87}Rb by Hoffmann-Pinther.¹³ The model used in these studies assumes one proton outside the neighboring lower mass Kr core. The energies and interactions of core states are taken from experiment whenever possible. The core-particle interaction is assumed to include dipole-dipole and quadrupole-quadrupole components.

The calculations done for ^{87}Rb (Ref. 13) included only the ground and first excited states of ^{86}Kr and ignored the $2d_{5/2}$ proton orbital. The parameters required are the energies and occupancies of the proton orbitals, the energy of the excited state of the Kr core, the magnitude of the two core-particle interactions and the reduced matrix elements of the quadrupole operator for the core. The one quantity for which no experimental guidance is currently available is the diagonal matrix element of the quadrupole operator for the excited state of the core. None of the 2^+ quadrupole moments are known experimentally.

Hoffmann-Pinther used the fact that several nuclei in this region have large excited-state moments and set this diagonal matrix element equal to the off-diagonal one. This procedure is supported by the results of elaborate Hartree-Fock calculations which reproduced the change in $B(E2)$ values across the Kr isotope chain and predicted reasonably large excited-state quadrupole moments.¹⁴ It is somewhat inconsistent to use such a matrix element with the physical 2^+ energy rather than finding an unperturbed core energy which combined with the quadrupole interaction reproduces the actual energy, but the effect is not that significant.

The distribution of spectroscopic strength in ^{86}Kr ($^3\text{He,d}$) ^{87}Rb is reasonably well reproduced by this calculation (see Table VII), although the splitting of strength in the $\frac{1}{2}^-$ and $\frac{9}{2}^+$ states is somewhat overpredicted.

The calculations performed for $^{83,85}\text{Rb}$ by Krishan, Basu, and Sen¹² included the second 0^+ , the second 2^+ ,

TABLE VIII. Summary of results for ($^3\text{He},d$) leading to Rb. $\langle E_x \rangle$ is the average excitation energy in keV weighted by G_{lj} .

		^{79}Rb	^{81}Rb	^{83}Rb	^{85}Rb	^{87}Rb
$3s_{1/2}$	G_{lj}	0.50	0.30	0.41	0.38	0.74
	$\langle E_x \rangle$	1321	2086	3095	4324	5825
$2p_{1/2}$	G_{lj}	1.65	2.58	2.67	2.25	2.41
	$\langle E_x \rangle$	437	434	311	871	1152
$2p_{3/2}$	G_{lj}	0.90	1.13	0.99	0.82	1.36
	$\langle E_x \rangle$	137	0	6	151	0
All $l=1$	G_{lj}	2.55	3.71	3.66	3.07	3.77
	$\langle E_x \rangle$	331	302	225	678	736
$2d_{5/2}$	G_{lj}	1.22	2.72	2.31	2.46	3.42
	$\langle E_x \rangle$	474	1686	2335	3776	5148
$1f_{5/2}$	G_{lj}	2.78	2.72	2.46	1.78	1.18
	$\langle E_x \rangle$	419	242	241	0	399
$1g_{9/2}$	G_{lj}	10.19	7.27	10.54	8.61	10.26
	$\langle E_x \rangle$	219	291	250	828	1636
	$G_{lj} (l=1,3,4)$	15.52	13.70	16.66	13.46	15.21
	$G_{lj} (\text{sum rule})$	12.86	13.33	13.64	13.85	14.00
	Difference	+ 17%	+ 3%	+ 18%	- 3%	+ 8%
	Max. E_x (keV)	2093	3302	3832	6185	6989

and the 4^+ , as well as the first 2^+ . This introduces several more core matrix elements for which there is no experimental guidance. The convention chosen was the procedure of Ford and Levinson.¹⁵ A few of the appropriate $B(E2)$ values are known for the very light isotopes and they indicate that this method may give matrix elements somewhat larger than would be derived from the experimental transition rates. However, the structure of the low-lying levels is relatively insensitive to the choice of these parameters. It should be noted that Krishen *et al.* did not scale these matrix elements with the square root of the appropriate $B(E2, 2^+ \rightarrow 0^+)$. Their value of the quadrupole coupling for ^{83}Rb was about 60% of that used for ^{85}Rb , roughly a factor of 2.5 less than the $B(E2)$ data would indicate. A $2d_{5/2}$ proton level was included in the calculation for ^{85}Rb . Calculated values of spectroscopic strengths for $^{83,85}\text{Rb}$ from Ref. 12 are listed in Tables V and VI. These calculations also overpredict the splitting of strength in the $\frac{1}{2}^-$ and $\frac{9}{2}^+$ states, with some derivations for other j 's as well. A more physical choice of core matrix elements would increase the splitting of the strength by increasing the mixing of core states, thus making the comparison with experiment even worse.

Consideration of the deformed nature of the Kr cores is clearly necessary in any attempt to describe the lighter Rb isotopes. Friederichs *et al.* studied ^{81}Rb using a model including Coriolis coupling.¹⁶ The first $\frac{1}{2}^-$ state is almost exclusively a proton in the Nilsson orbital $\frac{1}{2}[310]$, the first $\frac{3}{2}^-$ state is dominated by $\frac{3}{2}[312]$, and the first $\frac{5}{2}^-$ state is also mostly $\frac{3}{2}[312]$ with a small admixture of $\frac{1}{2}[310]$. The procedure for extracting particle-transfer strengths from Nilsson-model wave functions was given by Satchler.¹⁷ For the case of stripping onto a spin-zero target, the equations are particularly simple, including primarily the expansion of the Nilsson states in terms of spherical shell-model states. The latter expansion coefficients have been tabulated by Chi.¹⁸ Using the quoted value of $\beta=0.3$, the component of the $\frac{1}{2}[310]$ state with

$l=1, j=\frac{1}{2}$ is found to be less than 2%. This would imply an extremely small spectroscopic factor for this level, which is in dramatic disagreement with experiment. The $\frac{3}{2}[312]$ Nilsson state is about 9% $l=1, j=\frac{3}{2}$ and 81% $l=3, j=\frac{5}{2}$. These wave functions imply small spectroscopic strength for the $\frac{3}{2}^-$ level, also in disagreement with experiment. This calculation was done to fit the energies in one decoupled negative-parity band and thus does not represent a full calculation of the spectrum of ^{81}Rb . However, it does suggest that the model as applied in this case is in strong disagreement with the particle-transfer data.

One problem not considered in these calculations is that of exchange between the core and valence particles. It is clear from Kr(t,p) results^{4,19} that the excited states of the Kr isotopes are not exclusively two excited neutrons outside the ($A-2$) Kr core. If these states have appreciable components in which the core protons are excited, then the problem of exchange between the single odd proton and the excited protons in the core states becomes significant. A cluster calculation including several valence particles would partially avoid this difficulty. Such a calculation has been performed for ^{85}Rb .²⁰ In the absence of a consistent cluster calculation for the ground-state wave function of ^{84}Kr , spectroscopic factors can not be deduced from the published wave functions.

SUMMARY

Proton spectroscopic strengths for many levels in $^{79,81,83}\text{Rb}$ have been extracted using the $^{78,80,82}\text{Kr}(^3\text{He},d)$ reactions. In combinations with previous data, the present work provides a measure of the trends in the strength distribution across a spherical to deformed shape transition for the cores. Simple core-particle coupling models overpredict the splitting of strength among the low-lying levels. More sophisticated calculations, taking account of both the deformed nature of the lighter Kr isotopes and the possibility of proton excitations in the Kr excited

states are clearly needed. The results of the present study provide proton-orbital occupancies which are required as input to the calculations and also serves as a check of the strength distribution predicted by such models.

ACKNOWLEDGMENT

We acknowledge financial support from the National Science Foundation.

*Present address: Massachusetts Institute of Technology, Cambridge, MA 02139.

†Present address: Indiana University, Cyclotron Facility, Bloomington, IN 47405.

‡Present address: Drexel University, Philadelphia, PA 19104.

§Present address: Argonne National Laboratory, Argonne, IL 60439.

**Present address: State University of New York at Stony Brook, Stony Brook, NY 11794.

¹L. R. Medsker, J. N. Bishop, S. C. Headley, and H. T. Fortune, *Phys. Rev. C* **10**, 2117 (1974).

²L. R. Medsker, H. T. Fortune, S. C. Headley, and J. N. Bishop, *Phys. Rev. C* **12**, 1516 (1975).

³G. S. F. Stephans and H. T. Fortune, *Bull. Amer. Phys. Soc.* **27**, 498 (1982).

⁴G. S. F. Stephans, Ph.D. thesis, University of Pennsylvania, 1982 (unpublished).

⁵R. R. Betts, H. T. Fortune, and R. Middleton, *Phys. Rev. C* **8**, 660 (1973).

⁶J. R. Comfort, Argonne National Laboratory Report No. PHY-1970B, 1970 (unpublished).

⁷A. H. Wapstra and G. Audi, *Nucl. Phys.* **A432**, 55 (1985).

⁸P. D. Kunz (private communication).

⁹J. B. French and M. H. Macfarlane, *Nucl. Phys.* **26**, 168 (1961).

¹⁰J. Nag and M. K. Pal, *Nucl. Phys.* **A371**, 393 (1981).

¹¹V. K. B. Kota, S. P. Pandya, and V. Potbhare, *Phys. Rev. C* **25**, 1667 (1982).

¹²K. Krishan, S. K. Basu, and S. Sen, *Phys. Rev. C* **13**, 2055 (1976).

¹³P. Hoffmann-Pinther, *Z. Phys. A* **283**, 85 (1977).

¹⁴D. P. Ahalpara and K. H. Bhatt, *Phys. Rev. C* **25**, 2072 (1982).

¹⁵K. W. Ford and C. Levinson, *Phys. Rev.* **100**, 1 (1955).

¹⁶H. G. Friederichs, A. Gelberg, B. Heits, K. O. Zell, and P. von Brentano, *Phys. Rev. C* **13**, 2247 (1976).

¹⁷G. R. Satchler, *Ann. Phys.* **3**, 275 (1958).

¹⁸B. E. Chi, *Nucl. Phys.* **83**, 87 (1966).

¹⁹E. R. Flynn *et al.*, *Phys. Rev. C* **13**, 568 (1976).

²⁰R. A. Meyer *et al.*, *Phys. Rev. C* **21**, 2590 (1980).

²¹B. Singh and D. A. Viggars, *Nucl. Data Sheets* **37**, 393 (1982).

²²J. Müller, *Nucl. Data Sheets* **46**, 487 (1985).

²³D. C. Kocher, *Nucl. Data Sheets* **15**, 169 (1975).

²⁴W. Gast *et al.*, *Phys. Rev. C* **22**, 469 (1980).